

Observation of dopant-mediated intermixing at Ge/Si Interface

Hideki Takeuchi^{a)}

Department of Electrical Engineering and Computer Sciences, University of California at Berkeley, Berkeley, California 94720

Pushkar Ranade

Department of Materials Science and Engineering, University of California at Berkeley, Berkeley, California 94720

Vivek Subramanian and Tsu-Jae King

Department of Electrical Engineering and Computer Sciences, University of California at Berkeley, Berkeley, California 94720

(Received 29 October 2001; accepted for publication 26 March 2002)

Rapid intermixing of Ge deposited onto a Si substrate during 900 °C rapid thermal annealing was analyzed using secondary ion mass spectroscopy. In undoped Ge samples, a 50 nm thick graded $\text{Si}_{1-x}\text{Ge}_x$ layer was formed in 1 min, consuming 30 nm Ge and 20 nm Si. Negligible profile change was seen after an additional 1 min anneal. With dopants inside the deposited Ge layer, the extent of the intermixing is increased: For B doping, 30 nm Ge and 30 nm Si are consumed; for As doping, 5 nm Ge and 100 nm Si are consumed. In the case of B, Ge–B codiffusion from the $\text{Si}_{1-x}\text{Ge}_x/\text{Si}$ heterojunction edge was also observed. The p - n junction depth difference between the two dopants can be explained by the difference in their solubilities, while the Ge–B codiffusion is attributed to excess vacancies generated during the initial intermixing. © 2002 American Institute of Physics. [DOI: 10.1063/1.1480485]

$\text{Si}_{1-x}\text{Ge}_x$ has several promising applications in Si-based integrated-circuit technology.^{1–3} A fundamental understanding of Ge/Si interdiffusion behavior during high-temperature annealing is needed, however. In this letter, we report on the phenomenon of Ge/Si intermixing at 900 °C.

Samples were prepared by depositing 60 nm polycrystalline Ge (340 °C)⁴ and 20 nm SiO_2 (450 °C) films successively onto 4 in. Si wafers (n and p type; $\sim 6 \times 10^{14} \text{ cm}^{-3}$) using low-pressure chemical vapor deposition processes. Dopants were then implanted inside the Ge films [$^{11}\text{B}^+$, $5 \times 10^{15} \text{ cm}^{-2}$, 5 keV ($R_p=12.8 \text{ nm}$) or $^{75}\text{As}^+$, $5 \times 10^{15} \text{ cm}^{-2}$, 35 keV ($R_p=18.5 \text{ nm}$)]. A solid-phase crystallization anneal (350 °C, 6 h) was performed to minimize the effects of implantation-induced defects. The samples were then annealed at 900 °C in N_2 for 1 min and 2 min with ramping rates of 200 °C/s. Ge and dopant depth profiles were analyzed by secondary ion mass spectroscopy (SIMS) (CAMECA-4f double-focusing magnetic sector mass spectrometer with Cs^+ 2 keV). The depth scale was calculated by a sputtering rate calibrated with Si using a surface profilometer ($\sim 0.01 \text{ \AA/s}$), and the obtained Ge layer depth coincides well with a thickness by cross-sectional transmission electron microscopy. The depth origin was set at the original Ge/Si interface, where small peaks of dopant atoms created by ionization yield change can be found. Judging from the peak widths at the interfaces, ion-mixing effects were less than 4 nm.

Figure 1 shows the SIMS profiles of undoped Ge/Si samples after annealing. Formation of 50 nm graded $\text{Si}_{1-x}\text{Ge}_x$, with consumption of 30 nm Ge and 20 nm Si, can be observed after 1 min, and negligible profile change is seen

after an additional 1 min anneal, which is consistent with the slow diffusion of Ge in Si ($\sim 10^{-17} \text{ cm}^2/\text{s}$ @ 900 °C).⁶ Considering that intermixing of epitaxial Ge/Si takes place during annealing at 300 °C–800 °C,⁵ the initial profile change is not a diffusion driven by concentration gradients, but rather a rapid intermixing by strain originated from lattice mismatch at the Ge/Si interface. The Matano plane at which the total transported Ge atoms balance was found to be 5 nm from the original interface inside the Si. The shift indicates a larger flux of Si than that of Ge. This observation is consistent with results of low-temperature annealing of the amorphous Ge/Si system.⁷ Interestingly, the Ge profiles both above and below the original interface can be fitted with complementary error functions as shown in Fig. 1, indicating that the strain-relaxation structural change process may also follow Fick's law with concentration-independent diffusivities.

The presence of B drastically affects the Ge/Si intermix-

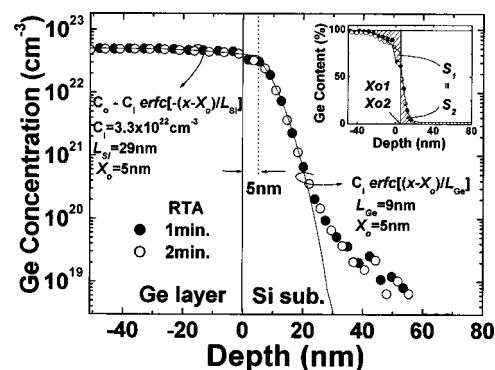


FIG. 1. Ge profiles after rapid thermal annealing of Ge/Si hetero structure at 900 °C. The two cross-hatched areas in the inset (S_1 and S_2) correspond to the total transported Ge atoms after annealing. $Xo1$, and $Xo2$, the positions of the Matano plane after 1 and 2 min annealing, are both 5 nm inside Si.

^{a)}Electronic mail: takeuchi@eecs.berkeley.edu

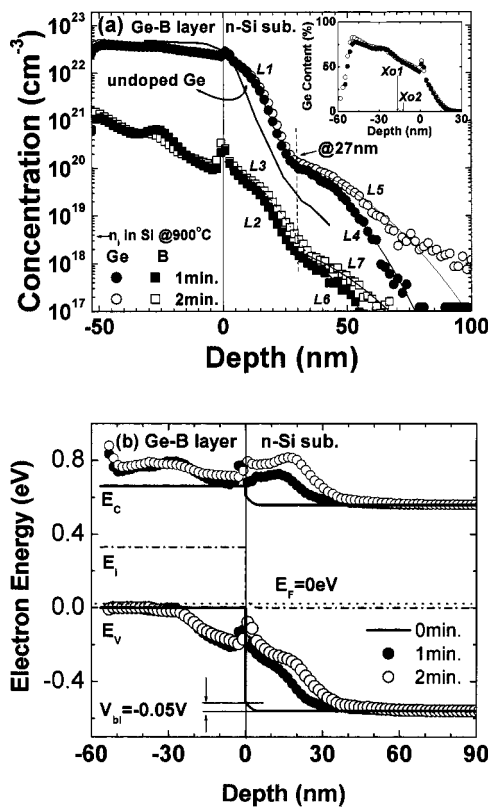


FIG. 2. (a) B and Ge depth profiles after 900 °C annealing of B-doped Ge/Si heterostructure. $Xo1$, and $Xo2$, the positions of the Matano plane after 1 and 2 min annealing, are 16.5 nm and 12.3 nm inside Ge, respectively. Li ($i = 1-7$) represent characteristic lengths of complementary error functions fitted to the measured data. $L1=13.7$ nm, $L2=15.5$ nm, $L3=18.5$ nm, $L4=20.5$ nm, $L5=28.7$ nm, $L6=21.0$ nm, and $L7=29.7$ nm. (b) Corresponding band diagrams at 900 °C calculated from the SIMS data.

ing behavior [Fig. 2(a)]. The Ge mole fraction varies almost linearly from the top surface ($\sim 80\%$) down to a depth 20 nm inside the Si substrate ($\sim 1\%$). The B profile decays in the vicinity of the original interface, and drops steeply inside the Si substrate. Kinks in concentration profiles are evident for Ge and B at the same depth of 27 nm inside the Si substrate. Similarly to the undoped samples, Ge and B profiles down to the depth of the kink show relatively small change with additional annealing. Inside the Si substrate, the Ge and B profiles can be fitted with complementary error functions, as labeled in Fig. 2(a) with characteristic lengths L_i . The characteristic lengths of Ge and B beyond the kink are very similar, and are proportional to the square root of the annealing time, suggesting that Ge-B codiffusion starts from the kink location, at time zero, with a diffusivity of 1.78×10^{-14} cm²/s, a factor of 45 higher than that of B in Si (3.9×10^{-16} cm²/s).⁸ Moreover, the B concentration at the kink, 2.0×10^{18} cm⁻³, is reasonably close to the intrinsic carrier concentration of Si at 900 °C (4×10^{18} cm⁻³).⁹

Band diagrams at 900 °C were plotted from the measured atomic concentrations, by assuming that the band gap and intrinsic carrier concentration of graded $Si_{1-x}Ge_x$ change linearly with Ge mole fraction, and by neglecting band-gap narrowing in heavily doped regions [Fig. 2(b)]. It can be seen that $p-n$ junctions were formed inside the graded $Si_{1-x}Ge_x$ layer. Considering that a B concentration below the intrinsic carrier concentration does not affect the Fermi en-

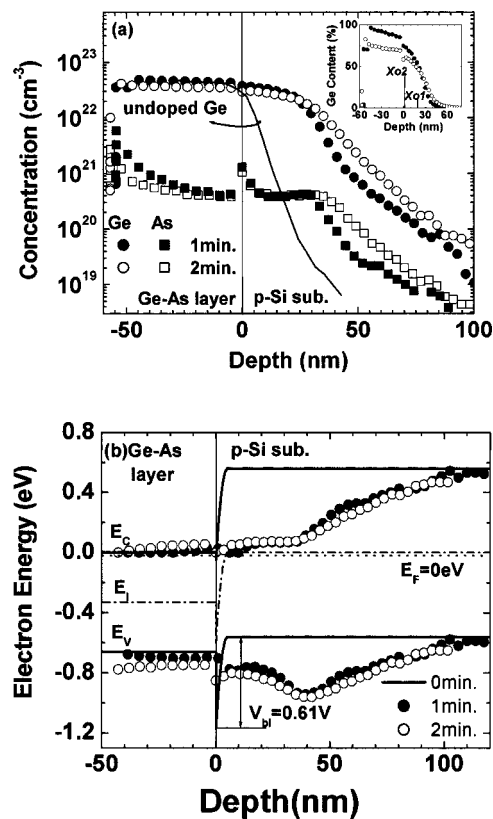


FIG. 3. (a) As and Ge depth profiles after 900 °C annealing of As-doped Ge/Si heterostructure. $Xo1$, and $Xo2$, the positions of the Matano plane after 1 and 2 min annealing, are 19.5 nm and 3.5 nm inside Si, respectively. (b) Corresponding band diagrams at 900 °C calculated from the SIMS data.

ergy, atomic transport in the region beyond the kink should be purely a diffusion process. Matano planes were found inside the original Ge layer, at 16.5 nm (after 1 min anneal) and 12.3 nm (after 2 min anneal). The shift in Matano plane position can be attributed to the existence of excess vacancies. Unbalanced fluxes of Si and Ge must generate excess vacancies in the Ge layer; a vacancy flux from Ge into Si, in turn, resulted, with accompanying Si atom transport into Ge. The vacancy flux also causes the Ge-B codiffusion starting at the depth of the kink.

Figures 3(a) and 3(b) show the Ge and As depth profiles and corresponding band diagrams, respectively. Again, $p-n$ junctions were formed in the graded $Si_{1-x}Ge_x$ layer. The flat As profile at 4×10^{20} cm⁻³ (between -50 and 50 nm) suggests that the deeper junction is due to the low solubility of As in Ge: Since As atoms can not be retained inside the Ge, they are transported deep into the Si codiffusing with Ge. Movement of the Matano plane, located on the Si side, from 19.7 (after 1 min anneal) to 3.5 nm (after 2 min anneal) is even more evident. At present, the factor that dominates the initial flux balance of Ge and Si is not clear. Differences in segregation tendency between n - and p -type dopants,¹⁰⁻¹² as well as the built-in potential polarity [indicated in Figs. 2(b) and 3(b)], should impact the atomic profiles, in addition to the solubility difference. Further study is necessary to clarify the mechanisms involved.

In conclusion, rapid intermixing of Ge and Si driven by strain results in a relatively thick graded $Si_{1-x}Ge_x$ layer. The Ge profile is strongly affected by dopants, and resultant $p-n$

junctions are confined inside the $\text{Si}_{1-x}\text{Ge}_x$. In the case of B-doped Ge, excess vacancies created during the initial structural change causes rapid Ge–B codiffusion. The confinement of dopant atoms within $\text{Si}_{1-x}\text{Ge}_x$ layers can be advantageous for the fabrication of ultrashallow junctions. A comprehensive analysis of diffusion phenomena will be crucial for the process optimization.

- ¹Y. C. Yeo, Q. Lu, T.-J. King, C. Hu, T. Kawachima, M. Oishi, S. Mashiro, and J. Sakai, *Tech. Dig. - Int. Electron Devices Meet.* **2000**, 753 (2000).
²K. Rim, S. Koester, M. Hargrove, J. Chu, P. M. Mooney, J. Ott, T. Kanarsky, P. Ronsheim, M. Jeong, A. Grill, and H.-S. P. Wong, *Proceedings of the 2001 Symposium on VLSI Tech. Dig.* (2001), p. 59.
³H. Takeuchi, W.-C. Lee, P. Ranade, and T.-J. King, *Tech. Dig. - Int. Electron Devices Meet.* **1999**, 501 (1999).
⁴A. Franke, D. Bilic, D. T. Chang, P. T. Jones, T.-J. King, R. T. Howe, and

- G. C. Johnson, *Proceedings of the IEEE International MEMS 1999 Conference*, Technical Digest (1999), p. 630.
⁵D. L. Kendall and D. B. DeVries, in *Semiconductor Silicon*, edited by R. R. Haberecht and E. L. Kern (Electrochemical Society, New York, 1969), p. 358.
⁶K. Nakajima, A. Konishi, and K. Kimura, *Phys. Rev. Lett.* **83**, 1802 (1999).
⁷A. Csik, D. L. Beke, G. A. Langer, Z. Erdelyi, L. Daroczi, K. Kaptan, and M. Kis-Varga, *Vacuum* **61**, 297 (2001).
⁸S. M. Sze, *Physics of Semiconductor Devices*, 2nd Ed. (Wiley, New York, 1981).
⁹R. N. Hall and W. C. Dunlap, *Phys. Rev.* **80**, 467 (1950).
¹⁰F. A. Trumbore, *Bell Syst. Tech. J.* **39**, 205 (1960).
¹¹S. M. Hu, D. C. Ahlgren, P. A. Ronsheim, and J. O. Chu, *Phys. Rev. Lett.* **67**, 1450 (1991).
¹²R. F. Lever, J. M. Bonar, and A. F. W. Willoughby, *J. Appl. Phys.* **83**, 1988 (1998).